



A novel approach to analyze the impact of lytic polysaccharide monooxygenases (LPMOs) on cellulosic fibres

Irina Sulaeva^a, David Budischowsky^b, Jenni Rahikainen^c, Kaisa Marjamaa^c, Fredrik Gjerstad Støpamo^d, Hajar Khaliliyan^b, Ivan Melikhov^b, Thomas Rosenau^b, Kristiina Kruus^{c,e}, Anikó Várnai^d, Vincent G.H. Eijssink^d, Antje Potthast^{b,*}

^a Core Facility "Analysis of Lignocellulosics" (ALICE), University of Natural Resources and Life Sciences, Vienna (BOKU), Konrad Lorenz-Straße 24, A-3430 Tulln an der Donau, Austria

^b Institute of Chemistry of Renewable Resources, Department of Chemistry, University of Natural Resources and Life Sciences, Vienna (BOKU), Konrad Lorenz-Straße 24, A-3430 Tulln an der Donau, Austria

^c Solutions for Natural Resources and Environment, VTT Technical Research Centre of Finland Ltd, Tietotie 2, FI-02044 Espoo, Finland

^d Faculty of Chemistry, Biotechnology and Food Science, NMBU - Norwegian University of Life Sciences, 1432 Ås, Norway

^e School of Chemical Engineering, Aalto University, P.O. Box 16100, Espoo 00076 AALTO, Finland

ARTICLE INFO

Keywords:

Cellulose
Oxidation
Solid fraction analysis
Size exclusion chromatography
Carbonyl

ABSTRACT

Enzymatic treatment of cellulosic fibres is a green alternative to classical chemical modification. For many applications, mild procedures for cellulose alteration are sufficient, in which the fibre structure and, therefore, the mechanical performance of cellulosic fibres are preserved. Lytic polysaccharide monooxygenases (LPMOs) bear a great potential to become a green reagent for such targeted cellulose modifications. An obstacle for wide implementation of LPMOs in tailored cellulose chemistry is the lack of suitable techniques to precisely monitor the LPMO impact on the polymer. Soluble oxidized cello-oligomers can be quantified using chromatographic and mass-spectrometric techniques. A considerable portion of the oxidized sites, however, remain on the insoluble cellulose fibres, and their quantification is difficult. Here, we describe a method for the simultaneous quantification of oxidized sites on cellulose fibres and changes in their molar mass distribution after treatment with LPMOs. The method is based on quantitative, heterogeneous, carbonyl-selective labelling with a fluorescent label (CCOA) followed by cellulose dissolution and size-exclusion chromatography (SEC). Application of the method to reactions of seven different LPMOs with pure cellulose fibres revealed pronounced functional differences between the enzymes, showing that this CCOA/SEC/MALS method is a promising tool to better understand the catalytic action of LPMOs.

1. Introduction

Irrefutable evidence of the negative changes in the worldwide environmental situation encourages the progressive development of green biorefinery strategies. A key issue in future bioeconomy scenarios is the increased use and valorization of renewable materials (Food and Agriculture Organization of the United Nations, 2017). For the bio-based industries to succeed in this development, reasonably priced and sustainable raw materials are needed. Wood cellulose, the major renewable product of forests, has a long utilization history, having been used for paper, paperboard, tissue, and fibre production for many decades. To a lesser extent, it is currently used for the production of

regenerated cellulose products, cellulose derivatives, and biofuels. At the same time, cellulose bears great potential for becoming one of the sustainable supermaterials of the future. The use of wood cellulose in textiles, packaging, and composites is an attractive alternative to fossil-based materials, synthetic polymers, and cotton, which suffer from adverse environmental impacts (Wang, Lu, & Zhang, 2016). Widely utilized polyester-based synthetic textiles have been continuously reported to represent one of the major sources of microplastic in the ocean (Browne, Dissanayake, Galloway, Lowe, & Thompson, 2008; Carney Almroth et al., 2018; Henry, Laitala, & Klepp, 2019), and so their replacement is expected to have a correspondingly benign environmental impact.

* Corresponding author.

E-mail address: antje.pothast@boku.ac.at (A. Potthast).

<https://doi.org/10.1016/j.carbpol.2023.121696>

Received 24 October 2023; Received in revised form 26 November 2023; Accepted 12 December 2023

Available online 14 December 2023

0144-8617/© 2023 The Authors. Published by Elsevier Ltd. This is an open access article under the CC BY license (<http://creativecommons.org/licenses/by/4.0/>).

The use of harsh chemicals in cellulose chemistry is still quite common due to the recalcitrant structure and hierarchical complexity of cellulose fibres. Cellulose polymer chains form microfibrils that are strongly fused by a network of hydrogen bonds (Heinze, 2015). Microfibrils are organized further into highly ordered, crystalline structures, which are found in native cellulose (cellulose I allomorph) as well as in regenerated fibres (cellulose II allomorph) and render at least parts of the polymer not readily accessible to chemical reagents and thus resistant to modification or derivatization (Heinze, El Seoud, & Koschella, 2018). Enzymes are natural tools that can be applied for cellulose modification, also of such less reactive regions, either as standalone enzymatic step or in combination with other chemical and physical treatments (Bayer, Chanzy, Lamed, & Shoham, 1998; Marjamaa & Kruus, 2018).

The most studied cellulose-targeting enzymes are cellulases, such as endo-acting endoglucanases and exo-acting cellobiohydrolases (Dashtban, Maki, Leung, Mao, & Qin, 2010). Cellulases are used to save energy in pulp refining, enhance pulp quality in terms of improved reactivity and accessibility, control the intrinsic viscosity, and adjust the molecular weight distribution (Gehmayer & Sixta, 2011; Jayasekara & Ratnayake, 2019). In the textile industry, cellulases are actively used to modify the fibre surface in processes named biopolishing, bioscouring, and biostonewashing, providing environmentally friendly alternatives to conventional, chemistry-driven, or otherwise polluting processes (Singh, 2016). Cellulases are also used for the activation and fibrillation of cellulose fibres in specific cellulose processing technologies, such as nanofibrillation (Hiltunen, Kemppainen, & Pere, 2013) or gel formation (Beaumont et al., 2016; Beaumont et al., 2019). Their standalone application on solid cellulose substrates is, however, rather limited – endoglucanases are known to hydrolyze the cellulose just partially, affecting primarily its amorphous part. Cellobiohydrolases can also act on crystalline cellulose, but their reaction rates are relatively low (Shrotri, Kobayashi, & Fukuoka, 2017).

Lytic polysaccharide monooxygenases (LPMOs) oxidize cellulose in both the crystalline (Beeson, Vu, Span, Phillips, & Marletta, 2015; Vaaje-Kolstad et al., 2010) and amorphous regions (Agger et al., 2014; Song et al., 2018; Vuong, Liu, Sandgren, & Master, 2017). Thus, they represent a novel type of enzymatic activity with the capability to modify the most recalcitrant celluloses (Eibinger et al., 2014). In contrast to cellulases, which are hydrolytic enzymes, LPMOs oxidize anhydroglucose units (AGUs) of the polysaccharides at the C1 and/or C4 positions utilizing either O₂ (Forsberg, 2019; Vaaje-Kolstad et al., 2010) or H₂O₂ (Bissaro et al., 2017; Filandr, 2020) as the oxidants (Chylenski et al., 2019). The oxidation leads to concomitant chain cleavage and the formation of a terminal lactone at the reducing end (C1-oxidized) and/or a 4-ketoaldopyranose at the non-reducing terminus (C4-oxidized) (Chylenski et al., 2019). The oxidized moieties disrupt the highly ordered crystalline structure (Eibinger et al., 2014; Song et al., 2018; Vermaas, Crowley, Beckham, & Payne, 2015). Therefore, LPMOs have the potential to be used for tailoring the properties of cellulosic fibres by altering the structural integrity of the fibres while introducing new oxidized functionalities on the fibre surface, which can possibly be employed in follow-up chemistry. While it is now clearly established that the addition of LPMOs to cellulolytic enzyme mixtures improves the saccharification of lignocellulosic biomass (Chylenski et al., 2019), their obvious ability to engineer cellulosic fibres still awaits exploration.

One bottleneck limiting the wider use of LPMOs in the biorefinery industry is the lack of methods for a precise estimation of their oxidative action and power (Eijsink et al., 2019). Upon LPMO treatment, usually, only a fraction of the cellulose fibre and its oxidized sites is released in the form of soluble cello-oligomers, whereas most oxidized sites remain within the insoluble fraction, situated at the fibre surface (Courtade, Forsberg, Heggset, Eijsink, & Aachmann, 2018; Wang, Li, Zheng, & Hsieh, 2021). The low molar mass degradation products can be quantitatively analyzed using common analytical techniques, including mass spectrometry and high-performance chromatographic approaches

(Wang et al., 2021; Westereng et al., 2018; Zweckmair et al., 2016). However, there is an obvious lack of analytical methodology covering the polymeric counterpart upon LPMO action on cellulosic substrates (Eijsink et al., 2019). The cellulose fraction is normally characterized using microscopic techniques that are not capable of providing detailed information on quantitative changes on the molecular level (Eibinger et al., 2014; Koskela et al., 2019). Alternatively, primarily insoluble oxidized products can be indirectly assessed after total hydrolysis (Courtade et al., 2018). This approach provides information on the total concentration of oxidized products, although there is interference from side reactions, and no localization of oxidized sites within the fibre can be derived.

The TTC (2,3,5 triphenyl-2H-tetrazolium chloride) assay may be used to approximate the aldehyde group content in cellulose (Obolenskaya, El'nitskaya, & Leonovich, 1991). In this method, the TTC reagent is reduced by an aldehyde group to colored formazan that can be quantified by colorimetry. A drawback of the method is that it operates at high alkalinity, which causes β -alkoxy elimination processes that will yield new reducing ends and thus increase the absolute number of aldehyde groups during the reaction (Hosoya, Bacher, Potthast, Elder, & Rosenau, 2018). However, TTC is usually able to show correct trends for cellulose oxidation with LPMOs (Ceccherini et al., 2021). In analogy to total hydrolysis, the method does not yield information on the localization of aldehydes nor on molar mass alterations of the substrate. Non-quantitative detection of newly formed oxidized sites on the substrate has been performed using X-ray photoelectron spectroscopy (XPS) (Selig et al., 2015) and through specific labeling with a fluorescence dye, 7-amino-1,3-naphthalenedisulfonic acid (ANDA) (Vuong et al., 2017). None of the methods tested, however, represents a robust approach to quantification of the oxidized sites and changes in the substrates' molar mass.

The primary goal of this study was to develop reliable analytical methodology for assessing the changes occurring in the cellulosic substrate during treatment with LPMOs, including variations in molar mass and molar mass-related distributions of carbonyl functions at the end and along the polymer chains, such as those introduced at C1 and/or C4 by the enzyme's action. A previously established method for monitoring such carbonyl profiles in relation to the molecular weight of cellulosic materials (Röhring et al., 2002a, 2002b) was adjusted to suit the requirements for characterisation of LPMO-treated fibres. Cellulose labeling with the carbonyl-selective fluorescence marker carbazole-9-carboxylic acid [2-(2-aminooxyethoxy)-ethoxy]-amide (CCOA) was performed to quantify the oxidized functionalities introduced upon treatment. The changes in molar mass distribution of the substrates were, in turn, monitored by size-exclusion chromatography (SEC) in combination with multi-angle light scattering/fluorescence/refractive index (MALS/FL/RI) detection (Henniges, Kostic, Borgards, Rosenau, & Potthast, 2011; Potthast et al., 2015). The established analytical protocol was validated for the evaluation of the insoluble cellulosic fraction generated in LPMO reactions in order to provide a missing piece of information regarding the function of LPMOs.

1.1. Hypothesis

The developed CCOA/SEC/MALS method provides a reliable and accurate approach for assessing the impact of Lytic Polysaccharide Monooxygenases (LPMOs) on non-soluble cellulosic substrates.

The method allows for the precise quantification of oxidized functionalities introduced by LPMOs, as well as changes in the molar mass distribution of the oxidized cellulose.

The method's application to various LPMO-reaction conditions reveals distinct functional differences among different LPMOs and enhances our understanding of their potential for tailored modification of cellulosic fibres.

2. Materials and methods

2.1. Enzymes

The LPMO enzymes *TrAA9A* from *Trichoderma reesei* (UniProt ID, O14405) and *PaAA9E* from *Podospora anserina* (UniProt ID, B2ATL7) were produced and purified as described in (Kont et al., 2019) and (Marjamaa et al., 2023), respectively. *NcAA9C* from *Neurospora crassa*, lacking the carbohydrate-binding module (CBM), i.e., *NcAA9C-N*, was produced in *Pichia pastoris* and purified as previously described (Borisova et al., 2015), with the following modifications. The recombinant yeast cells were incubated in BMGY medium at 29 °C, and the culture medium was supplemented with 1 % (v/v) glycerol (final concentration) each day. The culture broth was filtered and concentrated using a VivaFlow tangential crossflow concentrator (10,000 MWCO; Sartorius Stedim Biotech, Goettingen, Germany) and dialyzed against 20 mM Tris/HCl buffer, pH 8.0. The resulting protein solution was loaded on a 5 mL HiTrap DEAE FF column (GE Healthcare) with 20 mM Tris/HCl buffer, pH 8.0, at a flow rate of 2 mL/min. The flowthrough was collected, concentrated in 50 mM Bis-Tris/HCl buffer, pH 6.5, using 3000 MWCO PES centrifugal filters (Vivaspin; Sartorius Stedim Biotech), and then Cu²⁺-saturated by incubating with a three-fold molar excess of CuSO₄ for 20 min at 4 °C. Excess copper was removed by size exclusion chromatography using a HiLoad™ 16/600 Superdex™ 75 PG column (GE Healthcare Bio-Sciences AB, Uppsala, Sweden), using 50 mM Bis-Tris/HCl buffer, pH 6.5, containing 200 mM NaCl as the eluent. Fractions containing the pure protein were pooled, concentrated and dialyzed against 50 mM Bis-Tris/HCl buffer, pH 6.5, using 3000 MWCO PES centrifugal filters (Vivaspin; Sartorius Stedim Biotech), filter-sterilized using 0.22-µm-pore-size Millex-GV filters (Merck Millipore, Burlington, MA, USA), and stored at 4 °C.

Thielavia terrestris AA9E (*TtAA9E*; UniProt ID, D0VWZ9), *Lentinus similis* AA9A (*LsAA9A*; UniProt ID, A0A0S2GKZ1), *Thermoascus aurantiacus* AA9A (*TaAA9A*; UniProt ID, G3XAP7), and an AA9 LPMO from an unnamed organism (denoted as unAA9-1) were kindly provided as purified proteins by Novozymes. The protein concentrations were analyzed with the Bradford assay (Bradford, 1976) and BSA standards using BioRad's Bradford assay kit according to the manufacturer's instructions. The molar concentrations were calculated based on the protein molar masses.

2.2. Cellulose treatment with different LPMOs

Whatman No. 1 cellulose fibres were purchased from GE Healthcare (production site China, $M_w = 380$ kg/mol as measured by SEC/MALS in DMAc/LiCl using dn/dc of 0.140; details of the analysis are provided below). The material was treated with either unAA9-1, *LsAA9A*, *NcAA9C-N*, *PaAA9E*, *TaAA9A*, *TrAA9A*, or *TtAA9E* using 10 % (w/v) fibre consistency, 5 µM enzyme loading and 10 mM gallic acid (GA) in 50 mM Bis-Tris/HCl buffer, pH 6.5, with a total reaction volume of 1 mL. Each reaction was carried out in duplicate, using 100 mg fibres per reaction in 10 mL tubes. The reactions were performed at 30 °C for 24 h, using an Intelli-Mixer RM-2 (ELMI, Latvia) with settings u2 and 35 rpm for shaking. The reactions were terminated by placing the tubes in a boiling water bath for 5 min. 1 mL Milli-Q water was added to each of the tubes, followed by intense mixing by vortexing and centrifugation at 2882g for 15 min. One mL of clear sample was taken for analysis of soluble sugars, and the remaining supernatant was removed by pipetting. The fibres were resuspended in 2 mL of 1 % sodium dodecyl sulfate and heated in a boiling water bath for 5 min to remove adsorbed proteins. Solids and liquids were separated by centrifugation, and the solids were washed three times with 2 mL 80 % (v/v) aqueous ethanol and once with 2 mL Milli-Q water. Liquids and solids were separated by centrifugation and pipetting between each washing step. The fibres were stored in 0.5 mL 80 % ethanol at 4 °C prior to analysis.

2.3. Cellulose treatments with *TrAA9A* using varying reductant and hydrogen peroxide concentrations

Cellulose fibres were treated with *TrAA9A* using 2.5 % (w/v) fibre consistency and 0.75 µmol enzyme per gram of dry fibre. In each reaction, 0.5 g fibres (dry weight) were treated in 20 mL reaction volume. The enzymatic reactions were carried out in 50 mM sodium phosphate buffer pH 7.0 in 100 mL bottles placed in a 45 °C water bath supplied with a magnetic stirrer. The total reaction time was 3 h. The reductant (GA) was added in the reaction either in the beginning, as one batch (1 mM final concentration), or every 15 min in concentrations 15 or 30 µM (final concentrations after 3 h reaction time 180 µM and 360 µM, respectively). In another experiment, hydrogen peroxide was added to the reaction every 15 min to concentrations of 25 µM or 100 µM per addition, along with 15 µM GA. At the end of the reaction, the liquid was first removed by filtration through 60 µm mesh. After that, the liquid was filtered again through the fibres on the mesh cloth. The liquid collected after the second filtration was used for the sugar analyses. The fibres were washed with 100 mL Milli-Q water and freeze-dried for analysis.

2.4. Quantification of soluble oxidized products

Soluble oxidized products were treated with 1 µM *TrCel7A* from *T. reesei* (UniProt ID, G0RVK1) overnight at 37 °C to simplify the profile of C4-oxidized products to mainly Glc4gemGlc and Glc4gem(Glc)₂ and the profile of C1-oxidized products to GlcGlc1A, (Glc)₂Glc1A, and (Glc)₃Glc1A, as reported before (Forsberg et al., 2014; Petrović et al., 2019). The treated samples were analyzed and quantified by high-performance anion exchange chromatography with pulsed amperometric detection (HPAEC-PAD) using a Dionex ICS-5000 system equipped with CarboPac PA200 analytical (3 × 250 mm) and guard (3 × 50 mm) columns (Thermo Scientific, Sunnyvale, CA, USA), using a 26 min gradient protocol as previously described (Tuveng et al., 2020). GlcGlc1A, (Glc)₂Glc1A, and (Glc)₃Glc1A standards were produced by treating cellobiose, cellotriose, and cellotetraose with the cellobiose dehydrogenase *MtCDH* from *Myriococcum thermophilum* (UniProt ID, A9XK88) (Zámocký et al., 2008), while Glc4gemGlc and Glc4gem(Glc)₂ standards were prepared by treating cello-1,4-β-D-pentaose (Megazyme International, Ireland) with C4-oxidizing *NcAA9C* as previously described (Müller, Várnai, Johansen, Eijnsink, & Horn, 2015).

2.5. Carbonyl-selective fluorescence labelling of cellulose with CCOA

Selective labeling of carbonyl groups in enzymatically treated and untreated (negative control) cellulosic pulps was performed with the fluorescence marker CCOA according to Röhrling et al. (2002a, 2002b). Briefly, 20 mg of pulp (dry weight) was suspended in 2 mL of a stock solution of CCOA (125 mg/mL) in a 20 mM zinc acetate buffer (pH 4.0). The suspension was agitated in a water bath for 7 days at 40 °C. The labeled pulp was removed by filtration and thoroughly washed with Milli-Q water and 100 % ethanol.

2.6. Dissolution of CCOA-labelled cellulose for SEC analysis

The labeled pulp samples were subjected to a solvent exchange procedure (from ethanol to DMAc). Residual solvent was removed by filtration, and samples (appr. 15–20 mg of dry weight per sample) were placed into 2 mL of *N,N*-dimethylacetamide (DMAc)/LiCl (9 % w/v) for 24 h to achieve dissolution. The samples were filtered through a 0.45 µm syringe filter and subjected to SEC analysis (Röhrling et al., 2002a, 2002b).

2.7. SEC/MALS/FL/RI analysis

The SEC system consisted of the following components: HPLC pump

(G1312B; Agilent Technologies, Waldbronn, Germany), autosampler (G1367B; Agilent Technologies, Waldbronn, Germany), fluorescence detector (TSP 3000, Spectra Physics), MALS detector (Wyatt Dawn DSP with a diode laser, $\lambda = 488$ nm) and refractive index detector (Shodex RI-71). Four serial SEC columns, Styragel HMW6E Mixed Bed 20 μm , 7 \times 300 mm (Waters GmbH, Vienna, Austria), were used as the stationary phase. Operating conditions: 1.00 mL/min flow rate, 100 μL injection volume, and 45 min run time. DMAc/LiCl (0.9 %, w/v), filtered through a 0.02 μm filter, was used as eluent. Data were evaluated using Astra 4.7, Grams 7, Access, and OriginPro 2020 software. Two independent measurements were performed for each sample. The data are presented as average values of the two determinations.

The number of chain scissions per AGU can be estimated as $S = 1 / \text{DP}_n^0 - 1 / \text{DP}_n^t$, where DP_n^0 is the number-average degree of polymerization (DP), and DP_n^t is the number-average DP after S scissions have occurred (Calvini, 2010; Whitmore & Bogaard, 1994). To quantitatively correlate S with the content of carbonyl groups, S was expressed in terms of micromoles of scissions per gram of cellulose according to the equation $S_{\mu\text{mol/g}} = 6170 * (1 / \text{DP}_n^t - 1 / \text{DP}_n^0)$, where 6170 ($\mu\text{mol/g}$) is a conversion factor, the reciprocal value of the AGU's molecular weight ($M_{\text{AGU}} = 162.15$ g/mol = 0.000162 g/ μmol) (Calvini, 2010; Whitmore & Bogaard, 1994). The difference in carbonyl values between treated samples and the blank, i.e., $\Delta \text{C}=\text{O}$ ($\mu\text{mol/g}$), divided by S provides an estimated number of newly introduced functional groups formed per one chain scission – a parameter that reveals differences between C1- and C4-oxidizing LPMOs.

2.8. Statistical data analysis

A Multivariate Analysis, particularly Partial Least Squares Discriminant Analysis (PLS-DA), was employed for data classification purposes (Breton & Lloyd, 2014). The analysis used Matlab (version R2019b, Mathworks, Natick, MA, USA) and the PLS Toolbox (version 8.7, Eigenvector Research, Manson, WA, USA). The predictive performance of the developed models was assessed through a confusion matrix table. As a preprocessing step, the data were mean-centered. A Partial Least Squares Regression (PLS-R) technique was used to relate a set of input variables X (generated data on chain scissions S and carbonyl groups $\Delta \text{C}=\text{O}$ in combination with the known regioselectivity of LPMO) to a set of response variables Y (predicted sample class; defined in our case as

“C1”, “C4”, and “C1/C4”) (Breton & Lloyd, 2014). Samples were assigned to the classes if they exceeded a set threshold based, e.g., on the most probable prediction. The final predicted classification was assigned based on the highest predictive probability received. A model set for the different groups was built upon the results of 52 samples treated with C1-oxidizing LPMOs, 42 samples treated with C4-oxidizing LPMOs, and 43 samples treated with C1/C4 oxidizers. The detailed sample list is provided in Table S1. Adding the groups of C1 and C4 allowed for the prediction of major oxidized products left on cellulose upon treatment with C1/C4-oxidizing LPMOs.

3. Results and discussion

3.1. General concept

Oxidative cleavages of cellulose chains introduced by LPMOs lead to the formation of oxidized glucopyranose units at one of the two newly formed chain ends. LPMO action results in the formation of either a δ -lactone (in equilibrium with the corresponding aldonic acid) at the C1 position plus a new non-reducing end, or a 4-ketoaldose (in equilibrium with the corresponding hydrate, a geminal diol) at the C4 position plus a new reducing end (Fig. 1). Note that some LPMOs, including *TrAA9A* and *TaAA9A* used in this study, are not strictly C1-oxidizing or C4-oxidizing but produce mixtures of C1- and C4-oxidized products, which results in simultaneous generation of new non-reducing and reducing ends, respectively. Apart from that regular action mode, a certain amount of additional oxidized functional groups is expected to be introduced upon enzymatic treatment due to possible side activities of LPMOs (e.g., C6-oxidation (Bey et al., 2013; Chen et al., 2018; Sun et al., 2021)) and/or to non-specific oxidation, which may occur due to the presence of redox-active transition metal ions. In terms of newly introduced oxidized functionalities through the primary LPMO reaction, a C1-oxidizing LPMO would introduce one lactone (cyclic ester) functionality, whereas a C4-oxidizing LPMO would generate two carbonyls, the new reducing end (hemiacetal) and a ketone (hydrate) at C4. It needs to be emphasized that the side reactions mentioned above may introduce additional carbonyls and that the substrates used may already contain carbonyls that resulted from (abiotic) oxidation reactions.

If the quantification of carbonyls in LPMO-treated cellulosic substrates is to be introduced as a routine method, it needs to be reliable

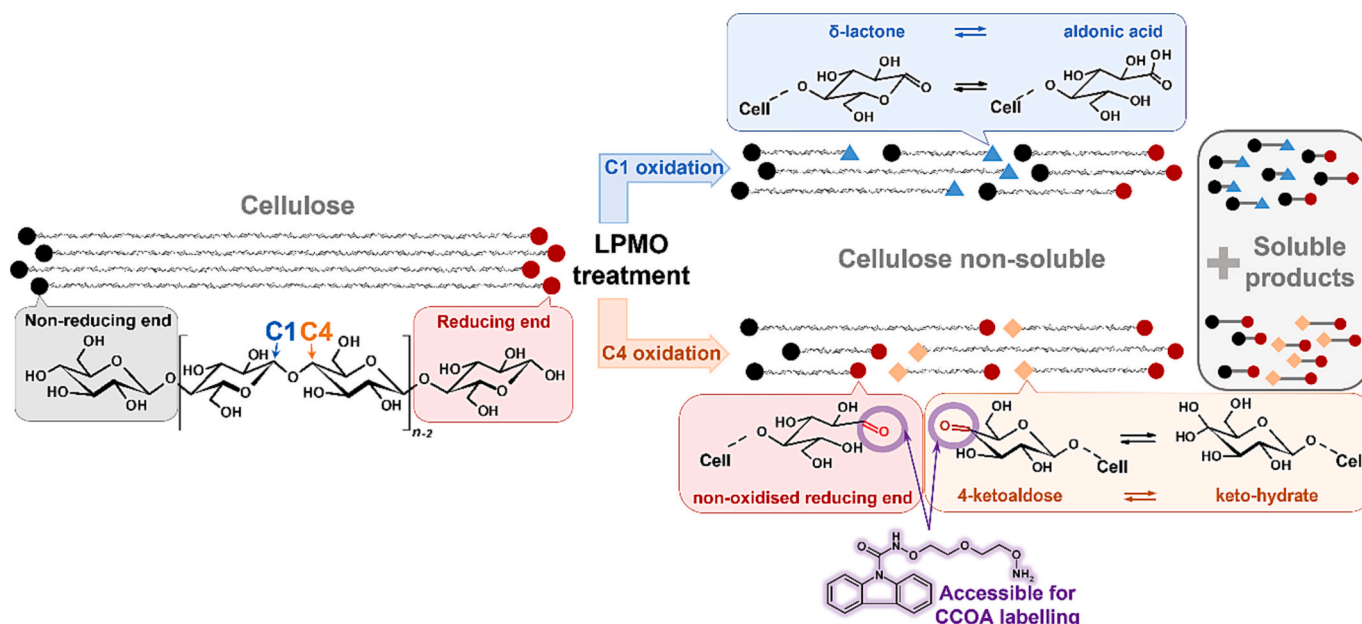


Fig. 1. Schematic representation of the LPMO enzymes' action on cellulose, resulting in chain cleavage and oxidation at C1 or C4 position.

over a broad range of carbonyl concentrations. From this viewpoint, the CCOA method, which covers carbonyl groups concentrations in the range 0.05 – 40 $\mu\text{mol/g}$ (Röhring et al., 2002a, 2002b) appears to be well suited for the analysis of LPMO-treated samples. The combination of the SEC/MALS analysis with the CCOA precolumn-labelling provides an especially powerful tool to get multifaceted insights into the LPMO action as it provides at the same time: a) information about changes in the cellulose's molar mass distribution, by the SEC/MALS analysis, b) data on the generation of carbonyl groups, by the fluorescence detection of CCOA-labelled carbonyl groups, and c) the profiles of carbonyl groups relative to the molar mass distribution, by combining the data from a) and b). The general advantages of the approach include its high sensitivity and the low amounts of sample material required (5–25 mg). Since CCOA is a carbonyl-specific label and hence does not react with C1-oxidized sites (i.e., carboxyl or lactone groups), the combination of CCOA-labelling and SEC-MALS offers, in addition, an opportunity to discriminate between C1- and C4-oxidations, since both cause chain cleavage (and thus decrease the molar mass) while only C4-oxidation generates the easy-to-label carbonyl groups as demonstrated in Fig. 1.

3.2. Formation of oxidized glucopyranose units in cellulose by different LPMOs

To obtain maximum sensitivity of the method, a Whatman No. 1 filter paper was used as the cellulose model substrate due to its purity and well-defined composition. Whatman No. 1 filter contains no hemicelluloses, which often carry oxidized groups from the production process that would distort the labelling results. It contains amorphous and crystalline areas different from PASC, which is a rather artificial substrate for LPMOs and has a molar mass that lies within the typical range of dissolving pulps and has not been artificially lowered by hydrolysis. To ensure the absence of residual proteins after LPMO treatment, which could potentially act as sites for carbonyl-selective labeling using CCOA and consequently contribute to the total C=O values, control experiments were performed. These controls involved the analysis of two blank samples – one with LPMO and another without LPMO. No reductant or oxygen donor was added to keep the enzyme silent. The results revealed no significant differences in the molar mass values nor the quantity of carbonyls in both blanks (Table S3). These tests confirmed that inactivated enzymes do not substantially contribute to the background values for C=O.

Table 1 shows the results of CCOA/SEC/MALS analyses of cellulose samples treated with a set of LPMOs, demonstrating how the different LPMO actions affect the molar mass distribution and the total amount of carbonyls. Fig. 2 shows the corresponding changes in the molar mass distributions and the carbonyl group profiles. Note again that all these

results refer to the polymeric, water-insoluble cellulose material, excluding the water-soluble monomer and oligomer fraction, as evident from the molar mass distributions.

The SEC analysis of the untreated Whatman No. 1 sample fully agreed with previously reported data (Henniges & Potthast, 2009). It was evident from Table 1 and Fig. 2 that all LPMO-treated samples have reduced molar masses, with the degree of molar mass loss depending on the enzyme used: Table 1 confirms a decrease in M_n , which translates into an increase in chain ends (S in Table 1), while Fig. 2 displays the corresponding shift in the molar mass distribution curves towards lower values. Likewise, all LPMO-treated samples showed an increase in carbonyl groups, which, expectedly, were much more pronounced for the C4-oxidizing LPMOs (see $\Delta\text{C=O}/S$ column in Table 1). SEC-MALS analysis (Fig. 2) showed the increase in carbonyls to be most prominent in the low-molar mass area. This fits well with the concept that LPMOs act on the surface of cellulose fibrils, where they cut individual chains multiple times, generating oligomers and polymer chains of varying lengths, while leaving the underlying chains less affected and largely intact.

The effects of the various LPMO treatments are further visualized in Fig. 3, which shows that the reduction in molar mass averages depends on the type of LPMO. *TtAA9E* and *NcAA9A-N* stand out by showing the largest reduction in M_w , by 17 % and 26 %, respectively. Of note, these differences may be relevant for the development of fibre processing strategies that aim at preserving the mechanical performance of cellulose. In this respect, a reaction that combines a small reduction in M_w with a high degree of oxidative modification could be beneficial, as is the case for, for example, *unAA9-1*.

3.3. Assessing LPMO mechanism of action

Cellulose degradation by LPMOs is accompanied by the release of oxidized soluble products, which emerge when a cellulose chain is cut near a chain end or when a chain is cut twice at positions that are only a few (<approx. 10) anhydroglucose units apart. Quantification of soluble sugars largely confirmed the anticipated oxidative regioselectivities and showed that the two C1/C4-oxidizing LPMOs primarily oxidize at the C4 position when acting on cellulose fibres (Fig. 4). Most remarkably, the amounts of released soluble products do not correlate with the degree of cellulose degradation, i.e., the generation of new chain ends in cellulose (see S in Table 1). This indicates larger variations in the way in which LPMOs attack the substrate. For example, an LPMO binding preferentially to regions with many chain ends could produce a plethora of soluble products while hardly reducing the overall molar mass of the cellulose. Likewise, LPMOs containing a CBM could be more “fixed” on the substrate, which would lead to many cleavages in a limited region,

Table 1

Results of SEC/MALS/FL/RI analysis of CCOA-labelled Whatman No. 1 paper samples treated with various LPMOs under otherwise identical conditions (see experimental part). The data represent an average value from two independent measurements; $\Delta\text{C=O}$ ($\mu\text{mol/g}$) denotes the difference in carbonyl values between treated samples and the blank; and S ($\mu\text{mol/g}$) indicates the number of chain scissions. $\Delta\text{C=O}/S$ reflects the number of newly introduced functional groups formed per one chain scission. The color codes represent the different oxidation modes of the LPMOs; it is used throughout the paper in the following figures.

| Sample | Enzyme oxidation mode | CBM | M_n , kDa | M_w , kDa | M_z , kDa | \bar{D} | Total C=O, $\mu\text{mol/g}$ | DP_n | $\Delta\text{C=O}$, mmol/100g | S , mmol/100g | $\Delta\text{C=O}/S$ |
|-----------------|-----------------------|-----|-------------|-------------|-------------|-----------|------------------------------|--------|--------------------------------|-----------------|----------------------|
| Blank | – | – | 180.3 | 382.5 | 626.6 | 2.12 | 0.49 | 1112 | – | – | – |
| <i>PaAA9E</i> | C1 | yes | 154.8 | 331.0 | 563.6 | 2.14 | 1.17 | 955 | 0.068 | 0.091 | 0.75 |
| <i>TtAA9E</i> | C1 | – | 143.7 | 317.8 | 534.3 | 2.21 | 2.87 | 887 | 0.238 | 0.141 | 1.69 |
| <i>LsAA9A</i> | C4 | – | 162.6 | 339.5 | 569.0 | 2.09 | 3.48 | 1003 | 0.299 | 0.061 | 4.90 |
| <i>NcAA9A-N</i> | C4 | – | 124.1 | 281.1 | 497.6 | 2.27 | 10.09 | 765 | 0.960 | 0.252 | 3.81 |
| <i>unAA9-1</i> | C4 | yes | 158.8 | 363.3 | 620.0 | 2.29 | 4.15 | 980 | 0.366 | 0.075 | 4.88 |
| <i>TrAA9A</i> | C1/C4 | yes | 153.7 | 358.8 | 611.2 | 2.33 | 2.19 | 948 | 0.170 | 0.095 | 1.79 |
| <i>TaAA9A</i> | C1/C4 | – | 159.5 | 351.8 | 595.2 | 2.21 | 3.92 | 984 | 0.343 | 0.073 | 4.70 |

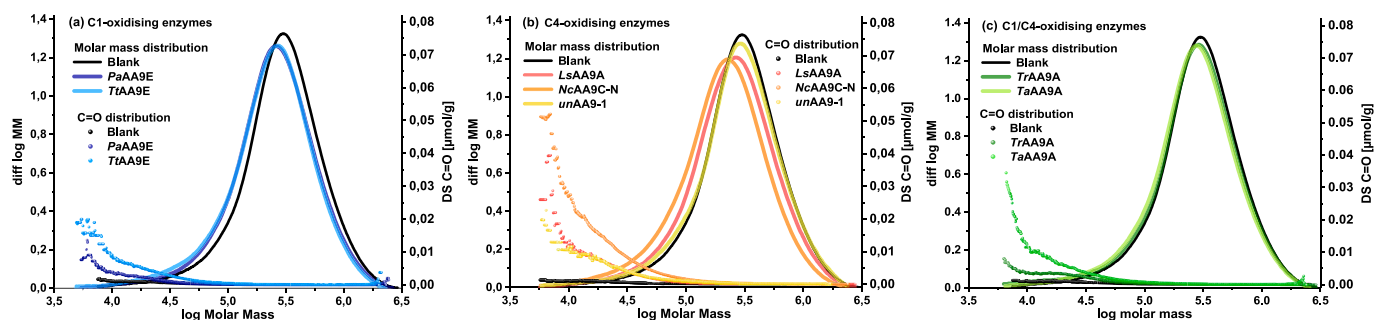


Fig. 2. Molar mass distribution profiles (left axes) and C=O distribution plots (right axes) of Whatman No. 1 cellulose treated with (a) C1-oxidizing, (b) C4-oxidizing, or (c) C1/C4-oxidizing LPMOs. The plots show the shift of molar mass distribution curves towards lower molar masses compared to the untreated starting material (blank), reflecting the degradation of cellulose polymeric chains caused by LPMO, and the increase in carbonyl groups (C=O) in the treated samples, showing their new formation upon LPMO treatment.

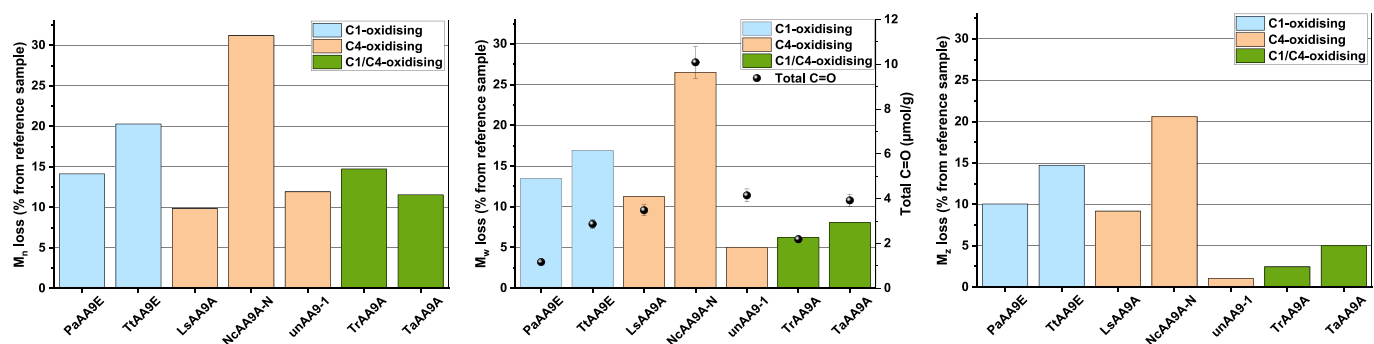


Fig. 3. Decrease of the statistical polymer parameters, M_n (left), M_w (middle), and M_z (right), shown in percent compared to the starting material (Whatman No. 1 cellulose). The middle graph shows also the total amounts of carbonyl groups. For the underlying data is shown in Table 1.

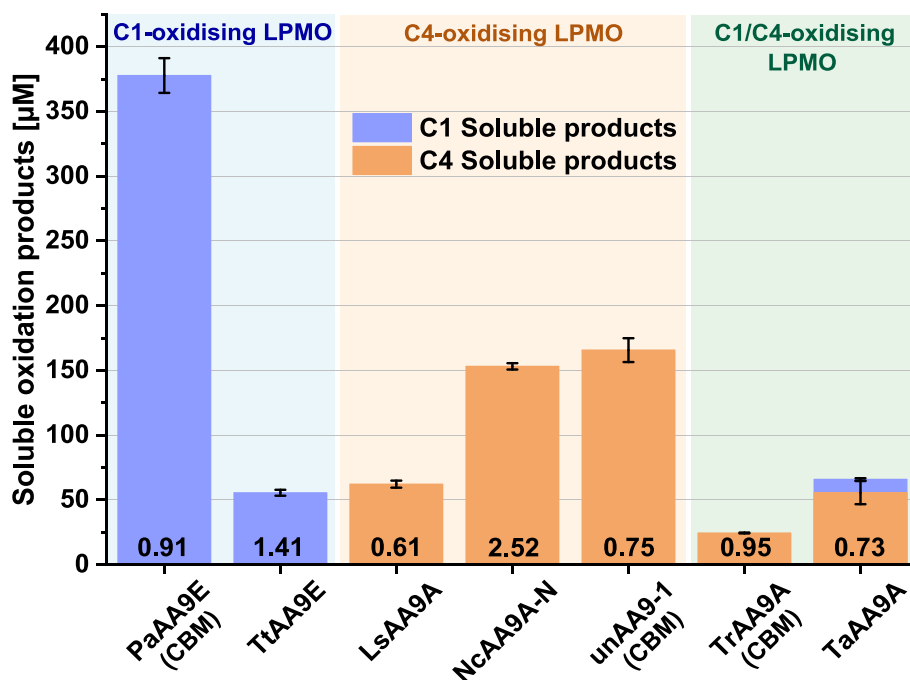


Fig. 4. The quantification of soluble oxidized products in the reactions is displayed in Table 1. The number written in the bars is the increase in chain ends, as derived from M_n values (i.e., the S values in Table 1).

which again would lead to the release of a larger number of solubles, as demonstrated by Courtade et al. for a C1-oxidizing bacterial LPMO (ScAA10A) (Courtade et al., 2018). Both scenarios could apply to CBM-containing PaAA9E, which produces much more soluble products

compared to other enzymes (Fig. 4), while the molar mass reduction of the solid fraction is not particularly high (Figs. 2–3). On the other hand, the CBM-free NcAA9C-N does generate only moderate amounts of soluble fragments but leads to more pronounced cellulose degradation. In

this case, the enzyme likely attacks longer polymeric chains in a more randomized manner, performing the oxidative cleavages at various positions away from chain ends. This mode of action would not always result in the formation of soluble oligomers but would significantly reduce the DP.

While these explanations are plausible, and while Fig. 4 reveals clear functional differences between cellulose-active LPMOs, generalization is not easily possible. Recent studies show that increased substrate binding is observed in the case of enzymes carrying a CBM, which in turn facilitates localized cellulose oxidations and promotes the formation of soluble sugars. In contrast, CBM-free LPMOs show enhanced mobility along the substrate and, therefore, less localized oxidations, which lead to lower amounts of soluble products and to enhanced formation of oxidized sites at cellulose (Courtade et al., 2018; Koskela et al., 2019).

In this study, three CBM-carrying enzymes were tested, *PaAA9A*, *unAA9A-1*, and *TrAA9A*, but only two of them (*PaAA9A* and *unAA9A-1*), showed the expected behavior, i.e., a high fraction of soluble products relative to the total number of cleavages at the cellulose backbone (Fig. 4). Likewise, the fraction of soluble products relative to the total amount of cuts also varies between the single domain LPMOs (Fig. 4). While the underlying mechanisms for the variations are not yet understood, it is clear that there must be variation in the way LPMO catalytic domains and CBMs bind to the substrate.

3.4. A closer look at the number of functional groups (C=O) produced per one chain scission

The ratio between the amount of carbonyl groups and the amount of chain scissions generated upon LPMO treatment (expressed as $\Delta C=O/S$ in Table 1) reveals the differences between C1- and C4-oxidizers. Alternatively, the specified parameter can be visualized as shown in Fig. 5, which illustrates data generated from a large sample set of 137 Whatman No. 1 samples that have been treated with a selection of

LPMOs with different regioselectivity (C1, C4, and C1/C4 oxidation) and modular structure (presence of CBM). Moreover, the dataset selected covers a variety of key treatment parameters (reaction time; reductant, co-substrate, feeding rates, and fibre consistency), which are essential for establishing a general model that is efficient in predicting the differences between C1- and C4-oxidizing LPMOs in a broad sample range. The overview of the treatment parameters is provided in the Supplementary material (Table S1).

According to the analysis, C1-oxidizing LPMOs may generate about 1 carbonyl per scission (data fit in Fig. 5 follows the corresponding trend line), whereas C4-oxidizing LPMOs and primarily C4-oxidizing LPMOs may generate up to 3 carbonyls per scission. The expected numbers of carbonyl groups detectable by the CCOA method are zero for C1 oxidation (as the CCOA label does not react with the carboxyl form and reacts only to a small degree with the lactone form of the newly formed carboxyl group) and two for C4 oxidation (as the CCOA label reacts with the newly formed reducing-end aldehyde and the 4-keto group at the nonreducing end), which suggests that additional oxidations take place, possibly due to the processes discussed above. These processes include possible side activities of LPMOs (e.g., C6-oxidation, hydrolysis), non-specific oxidation reactions occurring in the presence of a reductant and transition metal ions, and partial labeling of lactones in the case of C1-oxidation.

Fig. 5 shows a clear trend in data clustering depending on the enzymes' regioselectivities with a clear distinction between the clusters of C1- and C4-oxidizing LPMOs. The data points for C1/C4-oxidizers are scattered along these two clusters. For seven enzymes evaluated in this study, all data points appear within the expected regions in Fig. 5, except for a C1/C4-oxidizer *TrAA9A* that is grouped with the C1-oxidizing LPMOs. Next, the complete dataset consisting of 137 samples (Table S1) was subjected to PLS-DA analysis to build a model for predicting sample class membership (specified in our case as "C1", "C4" and "C1/C4") and, consequently, oxidized functionalities on cellulose after

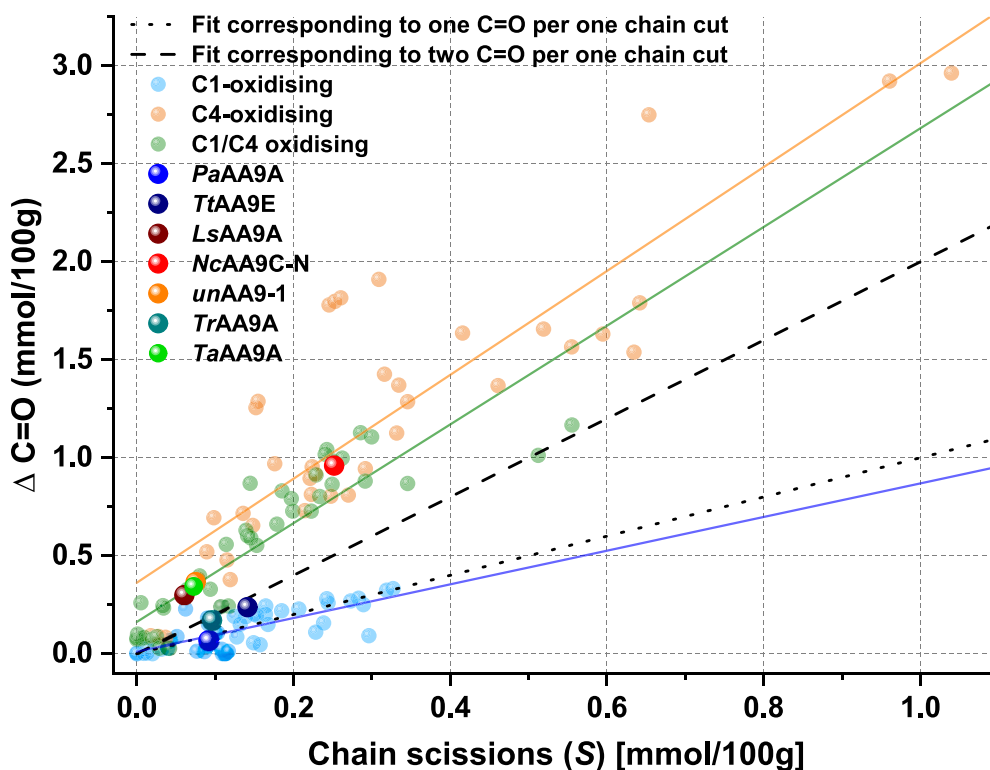


Fig. 5. Carbonyls versus chain scissions generated upon LPMO treatment. The dotted line represents a fit corresponding to one carbonyl group generated per one chain scission. The dashed line represents a fit corresponding to two carbonyl groups generated per one chain scission. The underlying data for a big dataset of 137 samples is shown in Table S1. The data for seven samples evaluated in this study are marked with corresponding color; the underlying data is shown in Table 1. (For interpretation of the references and color in this figure legend, the reader is referred to the web version of this article.)

LPMO treatment based on input variables ($\Delta C=O$ and S) in combination with the assay data (known regioselectivity of the enzymes). The PLS-DA analysis indicated a clear assignment of the samples to one of the three classes based on regioselectivity; the predicted classification is shown in Fig. S1b–d and summarized in Table S3. The model's prediction sensitivity and specificity parameters are shown in Table S2.

The model predicted C1 oxidation with good accuracy, placing C1-oxidizing LPMOs into the C1 cluster in 98 % and in the C1/C4 cluster in 2 % of the cases. However, the prediction of C4-oxidizing LPMOs showed less precision, with correct assignments to C4 oxidation in 67 % of cases and to C1/C4 oxidation in 31 % of cases. This outcome was expected, given that C4-oxidizing LPMOs largely overlapped with C1/C4-oxidizing enzymes. In the case of C1/C4-oxidizing LPMOs analyzed in this study, the PLS-DA analysis classified TrAA9A predominantly as C1-oxidizing and TaAA9A as performing oxidations at both C1 and C4 positions. While this prediction for TaAA9A aligned with the results of soluble fraction analysis; a suggestion that TrAA9A performs (predominantly) C1 oxidation contradicts the results of soluble fraction analysis (Fig. 4), which revealed the generation of almost exclusively C4-oxidized oligosaccharides by this LPMO. Considering that the C1/C4 product ratio may be very sensitive to minor variations in the geometry of the enzyme-substrate complex (Danneels, Tanghe, & Desmet, 2018; Forsberg, 2019), it is tempting to hypothesize that this LPMO might act near the reducing end of cellulose where it can solubilize shorter fragments with a C4 oxidation pattern while leaving longer cellulose chains with a C1-oxidized end in the insoluble fraction; this is, however, highly speculative. Coincidentally, this particular LPMO was used in further studies discussed below, and we note that these studies show higher ratios of carbonyl to cleavage sites under different reaction conditions, which is consistent with predominant C4 oxidation by TrAA9A (Table 2; next section).

3.5. Effect of reaction conditions on oxidative functionalization of cellulose fibres by TrAA9A

In cellulose oxidation reactions, LPMOs rely on the reducing power that reduces the enzyme's active-site copper to its catalytically active Cu (I) state, that drives the formation of H_2O_2 through reduction of O_2 . A vast variety of electron donors can serve as reductants, including partner enzymes (such as cellobiose dehydrogenase) or low molar mass compounds (e.g., ascorbic or gallic acid) (Frommhagen et al., 2016; Kracher et al., 2016; Kuusk et al., 2019; Stepnov et al., 2021). When hydrogen peroxide (H_2O_2) is supplied directly as a co-substrate, the reactions can be accelerated by several orders of magnitude (Danneels et al., 2018; Hangasky, Iavarone, & Marletta, 2018; Kuusk et al., 2018). At the same time, an excess of H_2O_2 might lead to enzyme damage due to self-oxidation (Bissaro et al., 2017). In reductant-driven reactions (i.e., no

externally added H_2O_2) the presence of free transition metal ions, such as Cu(II), may promote enzyme-independent H_2O_2 production resulting from oxidation of the reductant (Buettner & Jurkiewicz, 1996; Stepnov et al., 2021; Zhou et al., 2016).

From these previous studies, it is clear that the LPMO reaction rates and overall performance can be varied by changing the reductant, the co-substrate, or the substrate concentration. Much previous work has dealt only with the soluble products, which does not give a complete picture of the LPMO action. Therefore, we used CCOA/SEC/MALS to analyze the reaction of one of the LPMOs, TrAA9A, with Whatman No. 1 cellulose using varying reaction conditions. The conditions and the corresponding results of the CCOA/SEC/MALS analyses are shown in Table 2.

The data in Table 2 show that an increase in the amount of reductant and the controlled addition of H_2O_2 both promote cellulose degradation, which is reflected in a reduction of M_n and M_w and an increase of the total carbonyl content. Furthermore, substrate consistency in the reaction also plays a role in the extent of fibre oxidation as illustrated by the lower molar masses (M_n and M_w) and much higher carbonyl content ($\Delta C=O$ and $\Delta C=O/S$) reached when running the reaction with 1 mM reductant at 2.5 % consistency, compared to that with 10 mM reductant at 10 % consistency. In the former reaction, TrAA9A caused severe chain degradation with an overall M_n reduction of 58 % and a decrease in M_w of 11 % within the fairly short 3 h reaction time. In comparison, M_n and M_w decreased only by 27 % and 6.6 %, respectively, in the latter reaction after 24 h incubation (the underlying data is shown in Table 1). The reactions with gradual addition of both reductant and, in some cases, H_2O_2 show that lower amounts of reductant lead to less cellulose conversion and that the addition of H_2O_2 speeds up cellulose depolymerization (Fig. 6a). The difference in terms of molar mass reduction and formation of carbonyl groups on the fibre between the two tested H_2O_2 addition regimes was not that big, which probably indicates that in the reaction with the addition of the highest H_2O_2 amounts were saturating, which also means that enzyme inactivation may have occurred.

In the case of the lower consistency reactions depicted in Table 2, the obtained carbonyl versus scission ratios (Fig. 6b) were similar to those seen for C4-oxidizing LPMOs (Table 1, Fig. 5), in line with the expected predominating C4-oxidizing activity of TrAA9A (Fig. 4; Marjamaa et al., 2022). The formation of carbonyl groups relative to the chain scissions seemed to be somewhat lower at the highest reductant concentrations (1 and 10 mM) and at the higher substrate consistency. While we cannot explain this variation, the huge impact of consistency on the properties of fibres after LPMO treatment is worth noting. Importantly, the data in Table 2 show that the CCOA/SEC/MALS method allows for simultaneous monitoring of the functionalization and depolymerization of cellulose by LPMOs under different reaction conditions.

Table 2

CCOA/SEC/MALS analysis of reaction products generated after treating Whatman No. 1 cellulose with TrAA9A using different reaction conditions. Apart from the measured parameters, the following values were mathematically calculated: the difference in carbonyl values between treated samples and the blank ($\Delta C=O$, $\mu\text{mol/g}$); the number of chain scissions expressed in $\mu\text{mol/g}$ (S); and the parameter $\Delta C=O / S$ that reflects the number of newly introduced functional groups formed per one chain scission.

| Sample | Reductant (GA, μM) | H_2O_2 , μM | Reaction time, h | Dry matter content | M_n kDa | M_w kDa | M_z kDa | \bar{D} | Total C=O $\mu\text{mol/g}$ | DP_n | $\Delta C=O$ mmol/100 g | S mmol/100 g | $\Delta C=O / S$ |
|--------|--------------------------------|--------------------------|------------------|--------------------|-----------|-----------|-----------|-----------|-----------------------------|--------|-------------------------|----------------|------------------|
| Blank | – | – | – | 2.5 % | 210.5 | 384.0 | 588.5 | 1.82 | 0.78 | 1298 | – | – | – |
| Tr_1 | 180 ^a | – | 3 | 2.5 % | 180.2 | 362.1 | 578.6 | 2.01 | 4.75 | 1111 | 0.26 | 0.080 | 3.26 |
| Tr_2 | 180 ^a | 300 ^a | 3 | 2.5 % | 143.4 | 352.5 | 582.3 | 2.46 | 8.06 | 884 | 0.76 | 0.223 | 3.41 |
| Tr_3 | 180 ^a | 1200 ^a | 3 | 2.5 % | 138.1 | 340.4 | 585.3 | 2.33 | 9.43 | 852 | 0.89 | 0.249 | 3.57 |
| Tr_4 | 360 ^a | – | 3 | 2.5 % | 161.2 | 361.1 | 583.0 | 2.24 | 6.69 | 994 | 0.62 | 0.145 | 4.28 |
| Tr_5 | 1000 ^b | – | 3 | 2.5 % | 121.9 | 342.1 | 572.9 | 2.81 | 9.47 | 752 | 0.90 | 0.346 | 2.60 |
| TrAA9A | 10,000 ^b | – | 24 | 10 % | 153.7 | 358.8 | 611.2 | 2.33 | 2.19 | 948 | 0.170 | 0.095 | 1.79 |

^a GA was added every 15 min in an amount of either 15 μM or 30 μM per addition, which corresponds to a total concentration of 180 μM or 360 μM , respectively (the last addition was at $t = 2$ h 45 min). H_2O_2 was added every 15 min along with GA in an amount of 25 or 100 μM , which corresponds to a total concentration of 300 μM or 1200 μM , respectively (the last addition was at $t = 2$ h 45 min).

^b All GA was added in the beginning of the reaction; the reaction with 10,000 μM is the same reaction as shown in Table 1.

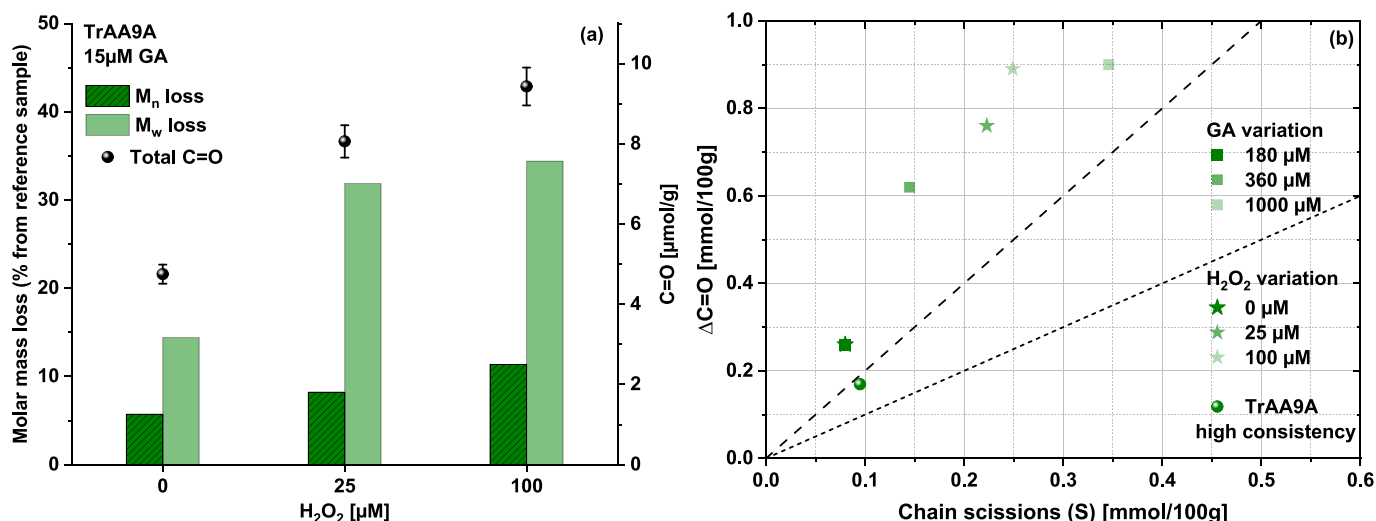


Fig. 6. CCOA/SEC/MALS analysis results after treating Whatman No. 1 cellulose with TrAA9A using different reaction conditions. (a): Changes in M_n , M_w , and the total amount of carbonyl groups for samples treated with TrAA9A depending on the concentration of a co-substrate H_2O_2 . The total concentration of the reductant (GA) is 180 μM in all experiments. (b): Carbonyls versus scissions generated upon treatment with TrAA9A under various reaction conditions. The dotted line represents the theoretical fit corresponding to one carbonyl group generated per one chain scission. The dashed line represents a fit corresponding to two carbonyl groups generated per one chain scission. The underlying data is shown in Table 2.

4. Concluding remarks

In this study, we have applied a CCOA/SEC/MALS approach for characterizing the impact of LPMO action on cellulosic substrates. We show that this method provides novel insight into the molar mass changes in the residual substrate, and, more importantly, towards the distribution of carbonyl groups along the molar mass profile of the oxidized cellulose. We also show that the method allows discriminating between the C1- and C4-oxidizing action of LPMOs. The method can universally be applied to different LPMO-reaction conditions and was used to show that variation in reductant levels or levels of externally added H_2O_2 have the expected effects on the degree of cellulose oxidation. The results for the various LPMOs tested, including the combined analysis of the soluble and insoluble reaction products, revealed large functional differences between the LPMOs. While the underlying causes of these functional differences remain largely unknown, they must relate to differences in the way the LPMOs target the substrate. These differences are important and need further studies since they may be relevant for the industrial implementation of LPMOs. Furthermore, such variation can help explain LPMO multiplicity in nature since it is conceivable that different LPMOs have evolved to target different types or parts of cellulose fibrils.

The method described herein not only provides a novel tool for determining the properties of LPMOs but also allows for more in-depth characterization of enzymatically treated celluloses. As such, this method may contribute to the future use of LPMOs in fibre processing and modification.

CRedit authorship contribution statement

Irina Sulaeva: Conceptualization, Data curation, Formal analysis, Writing – original draft, Writing – review & editing. **David Budischowsky:** Data curation, Formal analysis, Writing – review & editing. **Jenni Rahikainen:** Formal analysis, Investigation, Writing – review & editing, Project administration. **Kaisa Marjamaa:** Data curation, Formal analysis, Project administration, Writing – review & editing. **Fredrik Gjerstad Støpamo:** Investigation, Writing – review & editing. **Hajar Khaliliyan:** Data curation, Writing – review & editing. **Ivan Melikhov:** Formal analysis, Investigation, Writing – review & editing. **Thomas Rosenau:** Data curation, Writing – original draft, Writing – review &

editing, Resources. **Kristiina Kruus:** Formal analysis, Project administration, Writing – review & editing. **Anikó Várnai:** Data curation, Investigation, Project administration, Writing – original draft, Writing – review & editing, Supervision. **Vincent G.H. Eijssink:** Data curation, Funding acquisition, Project administration, Writing – original draft, Writing – review & editing, Supervision. **Antje Potthast:** Conceptualization, Data curation, Funding acquisition, Project administration, Supervision, Writing – original draft, Writing – review & editing.

Declaration of competing interest

The authors declare no competing financial interests.

Data availability

Data will be made available on request.

Acknowledgements

The financial support of ERA-NET Cofund Action “ForestValue” which includes the Academy of Finland (grant number 326359), the Research Council of Norway (grant agreement no. 297907) and the Austrian Federal Ministry of Agriculture, Forestry, Environment and Water Management (BMLFUW, Project 101379) is gratefully acknowledged. ForestValue has received funding from the European Union’s Horizon 2020 research and innovation program under grant agreement N° 773324. The support of the Austrian Biorefinery Center Tulln (ABCT-II) is gratefully acknowledged. The authors would like to thank Dr. Sonja Schiehsler for support with SEC measurements. VTT expresses gratitude to support by the FinnCERES Materials Bioeconomy Ecosystem and thanks Riitta Alander for technical assistance. NMBU also acknowledges financial support from the Research Council of Norway through the infrastructure grant 270038. Novozymes and Kasper Bay Tingsted and Pedro Loureiro are thanked for provision of enzymes and guidance for their use.

Appendix A. Supplementary data

Supplementary data to this article can be found online at <https://doi.org/10.1016/j.carbpol.2023.121696>.

References

- Agger, J. W., Isaksen, T., Várnai, A., Vidal-Melgosa, S., Willats, W. G., Ludwig, R., ... Westereng, B. (2014). Discovery of LPMO activity on hemicelluloses shows the importance of oxidative processes in plant cell wall degradation. *Proceedings of the National Academy of Sciences of the United States of America*, 111(17), 6287–6292. <https://doi.org/10.1073/pnas.1323629111>
- Bayer, E., Chanzy, H., Lamed, R., & Shoham, Y. (1998). Cellulose, cellulases and cellulosomes. *Current Opinion in Structural Biology*, 8(5), 548–557. [https://doi.org/10.1016/S0959-440X\(98\)80143-7](https://doi.org/10.1016/S0959-440X(98)80143-7)
- Beaumont, M., Rennhofer, H., Opjetnik, M., Lichtenegger, H., Potthast, A., & Rosenau, T. (2016). Nanostructured cellulose II gel consisting of spherical particles. *ACS Sustainable Chemistry & Engineering*, 4(8), 4424–4432. <https://doi.org/10.1021/acssuschemeng.6b01036>
- Beaumont, M., Rosenfeldt, S., Tardy, B., Gussenbauer, C., Khakalo, A., Opjetnik, M., ... Rosenau, T. (2019). Soft cellulose II nanospheres. Sol-gel behavior, swelling and material synthesis. *Nanoscale*, 11(38), 17773–17781. <https://doi.org/10.1039/c9nr05309c>
- Beeson, W., Vu, V., Span, E., Phillips, C., & Marletta, M. (2015). Cellulose degradation by polysaccharide monoxygenases. *Annual Review of Biochemistry*, 84, 923–946. <https://doi.org/10.1146/annurev-biochem-060614-034439>
- Bey, M., Zhou, S., Poidevin, L., Henrissat, B., Coutinho, P., Berrin, J.-G., & Sigoillot, J.-C. (2013). Cello-oligosaccharide oxidation reveals differences between two lytic polysaccharide monoxygenases (family GH61) from *Podospora anserina*. *Applied and Environmental Microbiology*, 79(2), 488–496. <https://doi.org/10.1128/AEM.02942-12>
- Bissaro, B., Röhr, A. K., Müller, G., Chylenski, P., Skaugen, M., Forsberg, Z., ... Eijsink, V. G. H. (2017). Oxidative cleavage of polysaccharides by monooxygenases depends on H₂O₂. *Nature Chemical Biology*, 13, 1123–1128. <https://doi.org/10.1038/nchembio.2470>
- Borisova, A., Isaksen, T., Dimarogona, M., Kognole, A., Mathiesen, G., Várnai, A., ... Eijsink, V. G. H. (2015). Structural and functional characterization of a lytic polysaccharide monoxygenase with broad substrate specificity. *Journal of Biological Chemistry*, 290(38), 22955–22969. <https://doi.org/10.1074/jbc.M115.660183>
- Bradford, M. (1976). A rapid and sensitive method for the quantitation of microgram quantities of protein utilizing the principle of protein-dye binding. *Analytical Biochemistry*, 72(2), 248–254. <https://doi.org/10.1006/abio.1976.9999>
- Brereton, R., & Lloyd, G. (2014). Partial least squares discriminant analysis: Taking the magic away. *Journal of Chemometrics*, 28(4), 213–225. <https://doi.org/10.1002/cem.2609>
- Browne, M., Dissanayake, A., Galloway, T., Lowe, D., & Thompson, R. (2008). Ingested microscopic plastic translocates to the circulatory system of the mussel, *Mytilus edulis* (L.). *Environmental Science & Technology*, 42(13), 5026–5031. <https://doi.org/10.1021/es800249a>
- Buettner, G., & Jurkiewicz, B. A. (1996). Catalytic metals, ascorbate and free radicals: Combinations to avoid. *Radiation Research*, 145(5), 532–541. <https://doi.org/10.2307/3579271>
- Calvini, P. (2010). What went wrong with the kinetics of cellulose degradation? In A. Lejeune, & T. Deprez (Eds.), *Cellulose: Structure and properties, derivatives and industrial uses* (pp. 417–426). New York: Nova Science Publishers Inc.
- Carney Almröth, B. M., Åström, L., Roslund, S., Petersson, H., Johansson, M., & Persson, N.-K. (2018). Quantifying shedding of synthetic fibers from textiles; a source of microplastics released into the environment. *Environmental Science and Pollution Research*, 25, 1191–1199. <https://doi.org/10.1007/s11356-017-0528-7>
- Ceccherini, S., Rahikainen, J., Marjamaa, K., Sawada, D., Grönqvist, S., & Maloney, T. (2021). Activation of softwood Kraft pulp at high solids content by endoglucanase and lytic polysaccharide monoxygenase. *Industrial Crops and Products*, 166, Article 113463. <https://doi.org/10.1016/j.indcrop.2021.113463>
- Chen, C., Chen, J., Geng, Z., Wang, M., Liu, N., & Li, D. (2018). Regioselectivity of oxidation by a polysaccharide monoxygenase from *Chaetomium thermophilum*. *Biotechnology for Biofuels*, 11, 155. <https://doi.org/10.1186/s13068-018-1156-2>
- Chylenski, P., Bissaro, B., Sørle, M., Röhr, A., Várnai, A., Horn, S., & Eijsink, V. G. H. (2019). Lytic polysaccharide monoxygenases in enzymatic processing of lignocellulosic biomass. *ACS Catalysis*, 9(6), 4970–4991. <https://doi.org/10.1021/acscatal.9b00246>
- Courtade, G., Forsberg, Z., Heggset, E. B., Eijsink, V. G. H., & Aachmann, F. L. (2018). The carbohydrate-binding module and linker of a modular lytic polysaccharide monoxygenase promote localized cellulose oxidation. *Journal of Biological Chemistry*, 293(34), 13006–13015. <https://doi.org/10.1074/jbc.RA118.004269>
- Danneels, B., Tanghe, M., & Desmet, T. (2018). Structural features on the substrate-binding surface of fungal lytic polysaccharide monoxygenases determine their oxidative regioselectivity. *Biotechnology Journal*, 14(3), Article 1800211. <https://doi.org/10.1002/biot.201800211>
- Dashtban, M., Maki, M., Leung, K., Mao, C., & Qin, W. (2010). Cellulase activities in biomass conversion: Measurement methods and comparison. *Critical Reviews in Biotechnology*, 30(4), 302–309. <https://doi.org/10.3109/07388551.2010.490938>
- Eibinger, M., Ganner, T., Bubner, P., Rosker, S., Kracher, D., Haltrich, D., ... Nidetzky, B. (2014). Cellulose surface degradation by a lytic polysaccharide monoxygenase and its effect on cellulase hydrolytic efficiency. *Journal of Biological Chemistry*, 289, 35929–35938. <https://doi.org/10.1074/jbc.M114.602227>
- Eijsink, V. G. H., Petrovic, D., Forsberg, Z., Mekasha, S., Röhr, A., Várnai, A., Bissaro, B., & Vaaje-Kolstad, G. (2019). On the functional characterization of lytic polysaccharide monoxygenases (LPMOs). *Biotechnology for Biofuels and Bioproducts*, 12, 58. <https://doi.org/10.1186/s13068-019-1392-0>
- Filandr, F. (2020). The H₂O₂-dependent activity of a fungal lytic polysaccharide monoxygenase investigated with a turbidimetric assay. *Biotechnology for Biofuels and Bioproducts*, 13, 37. <https://doi.org/10.1186/s13068-020-01673-4>
- Towards sustainable bioeconomy guidelines. Retrieved from. Food and Agriculture Organization of the United Nations (FAO). <http://www.fao.org/3/ca5145en/ca5145en.pdf>, (2017).
- Forsberg, Z. (2019). Polysaccharide degradation by lytic polysaccharide monoxygenases. *Current Opinion in Structural Biology*, 59, 54–64. <https://doi.org/10.1016/j.sbi.2019.02.015>
- Forsberg, Z., Mackenzie, A. K., Sørle, M., Röhr, Å. K., Helland, R., Arvai, A. S., Vaaje-Kolstad, G., & Eijsink, V. G. H. (2014). Structural and functional characterization of a conserved pair of bacterial cellulose-oxidizing lytic polysaccharide monoxygenases. *Proceedings of the National Academy of Sciences of the United States of America*, 111(23), 8446–8451. <https://doi.org/10.1073/pnas.1402771111>
- Frommhamen, M., Koetsier, M., Westphal, A., Visser, J., Hinz, S., Vincken, J., van Berkel, W. J., Kabel, M. A., & Gruppen, H. (2016). Lytic polysaccharide monoxygenases from *Myceliophthora thermophila* C1 differ in substrate preference and reducing agent specificity. *Biotechnology for Biofuels and Bioproducts*, 9(1), 186. <https://doi.org/10.1186/s13068-016-0594-y>
- Gehmayr, V., & Sixta, H. (2011). Dissolving pulps from enzyme treated kraft pulps for viscose application. *Lenzinger Berichte*, 89, 152–160.
- Hangasky, J. A., Iavarone, A. T., & Marletta, M. A. (2018). Reactivity of O₂ versus H₂O₂ with polysaccharide monoxygenases. *Proceedings of the National Academy of Sciences of the United States of America*, 115(19), 4915–4920. <https://doi.org/10.1073/pnas.1801153115>
- Heinze, T. (2015). Cellulose: Structure and properties. In O. J. Rojas (Ed.), *Cellulose chemistry and properties: Fibers, nanocelluloses and advanced materials* (pp. 1–52). Springer International Publishing Switzerland. https://doi.org/10.1007/978-3-319-122015-3_19
- Heinze, T., El Seoud, O. A., & Koschella, A. (2018). Cellulose activation and dissolution. In T. Heinze, O. A. El Seoud, & A. Koschella (Eds.), *Cellulose derivatives. Synthesis, structure, and properties* (pp. 173–257). Springer International Publishing. https://doi.org/10.1007/978-3-319-73168-1_3
- Henniges, U., Kostic, M., Borgards, A., Rosenau, T., & Potthast, A. (2011). Dissolution behaviour of different celluloses. *Biomacromolecules*, 12(4), 871–879. <https://doi.org/10.1515/refer.017>
- Henniges, U., & Potthast, A. (2009). Bleaching revisited: Impact of oxidative and reductive bleaching treatments on cellulose and paper. *Restaurator*, 30(4), 294–320.
- Henry, B., Laitala, K., & Klepp, I. (2019). Microfibres from apparel and home textiles: Prospects for including microplastics in environmental sustainability assessment. *Science of the Total Environment*, 652, 483–494. <https://doi.org/10.1016/j.scitotenv.2018.10.166>
- Hiltunen, J., Kempainen, K., & Pere, J. (2013). *Process for producing fibrillated cellulose material Patent US10087477B2*. United States Patent.
- Hosoya, T., Bacher, M., Potthast, A., Elder, T., & Rosenau, T. (2018). Insights into degradation pathways of oxidized anhydroglucose units in cellulose by β-alkoxy-elimination: A combined theoretical and experimental approach. *Cellulose*, 25(7), 3797–3814. <https://doi.org/10.1007/s10570-018-1835-y>
- Jayasekara, S., & Ratnayake, R. (2019). Microbial Cellulases: An overview and applications. In A. R. Pascual, & M. E. E. Martín (Eds.), *Cellulose*. London: IntechOpen. <https://doi.org/10.5772/intechopen.84531>
- Kont, R., Pihlajaniemi, V., Borisova, A. S., Aro, N., Marjamaa, K., Loogen, J., Büchs, J., Eijsink, V. G. H., Kruus, K., & Våljamäe, P. (2019). The liquid fraction from hydrothermal pretreatment of wheat straw provides lytic polysaccharide monoxygenases with both electrons and H₂O₂ co-substrate. *Biotechnology for Biofuels and Bioproducts*, 12, 235. <https://doi.org/10.1186/s13068-019-1578-5>
- Koskela, S., Wang, S., Xu, D., Yang, X., Li, K., Berglund, L. A., ... Zhou, Q. (2019). Lytic polysaccharide monoxygenase (LPMO) mediated production of ultra-fine cellulose nanofibres from delignified softwood fibres. *Green Chemistry*, 21, 5924–5933. <https://doi.org/10.1039/C9GC02808K>
- Kracher, D., Scheiblbrandner, S., Felice, A. K., Breslmayr, E., Preims, M., Ludwicka, K., ... Ludwig, R. (2016). Extracellular electron transfer systems fuel cellulose oxidative degradation. *Science*, 352, 6289. <https://doi.org/10.1126/science.aaf3165>
- Kuus, S., Bissaro, B., Kuusk, P., Forsberg, Z., Eijsink, V. G. H., Sørle, M., & Våljamäe, P. (2018). Kinetics of H₂O₂-driven degradation of chitin by a bacterial lytic polysaccharide monoxygenase. *Journal of Biological Chemistry*, 293(2), 523–531. <https://doi.org/10.1074/jbc.M117.817593>
- Kuus, S., Kont, R., Kuusk, P., Heering, A., Sørle, M., Bissaro, B., Eijsink, V. G. H., & Våljamäe, P. (2019). Kinetic insights into the role of the reductant in H₂O₂-driven degradation of chitin by a bacterial lytic polysaccharide monoxygenase. *Journal of Biological Chemistry*, 294(5), 1516–1528. <https://doi.org/10.1074/jbc.RA118.006196>
- Marjamaa, K., & Kruus, K. (2018). Enzyme biotechnology in degradation and modification of plant cell wall polymers. *Physiologia Plantarum*, 164(1), 106–118. <https://doi.org/10.1111/ppl.12800>
- Marjamaa, K., Lahtinen, P., Arola, S., Maiorova, N., Nygren, H., Aro, N., & Koivula, A. (2023). Oxidative treatment and nanofibrillation softwood kraft fibres with lytic polysaccharide monoxygenases from *Trichoderma reesei* and *Podospora anserina*. *Industrial Crops and Products*, 193, Article 116243. <https://doi.org/10.1016/j.indcrop.2023.116243>
- Marjamaa, K., Rahikainen, J., Karjalainen, M., Maiorova, N., Holopainen-Mantila, U., Molinier, M., Aro, N., Nygren, H., Mikkelsen, A., Koivula, A., & Kruus, K. (2022). Oxidative modification of cellulosic fibres by lytic polysaccharide monoxygenase AA9A from *Trichoderma reesei*. *Cellulose*, 29, 6021–6038. <https://doi.org/10.1007/s10570-022-04648-w>

- Müller, G., Várnai, A., Johansen, K., Eijsink, V. G. H., & Horn, S. (2015). Harnessing the potential of LPMO-containing cellulase cocktails poses new demands on processing conditions. *Biotechnology for Biofuels and Bioproducts*, 8, 187. <https://doi.org/10.1186/s13068-015-0376-y>
- Obolenskaya, A. V., El'nitskaya, Z. P., & Leonovich, A. A. (1991). Laboratory work in the chemistry of wood and cellulose. *Ecology*, 7, 78–155.
- Petrović, D., Várnai, A., Dimarogona, M., Mathiesen, G., Sandgren, M., Westereng, B., & Eijsink, V. G. H. (2019). Comparison of three seemingly similar lytic polysaccharide monoxygenases from *Neurospora crassa* suggests different roles in plant biomass degradation. *Journal of Biological Chemistry*, 294(41), 15068–15081. <https://doi.org/10.1074/jbc.RA119.008196>
- Pothast, A., Radosta, S., Saake, B., Lebioda, S., Heinze, T., Henniges, U., Isogai, A., Koschella, A., Kosma, P., Rosenau, T., Schiehsler, S., Sixta, H., Strlic, M., Strobin, G., Vorwerg, W., & Wetzel, H. (2015). Comparison testing of methods for gel permeation chromatography of cellulose: Coming closer to a standard protocol. *Cellulose*, 22(3), 1591–1613. <https://doi.org/10.1007/s10570-015-0586-2>
- Röhring, J., Pothast, A., Rosenau, T., Lange, T., Borgards, A., Sixta, H., & Kosma, P. (2020a). A novel method for the determination of carbonyl groups in celluloses by fluorescence labeling. 2. Validation and applications. *Biomacromolecules*, 3(5), 969–975. <https://doi.org/10.1021/bm020030p>
- Röhring, J., Pothast, A., Rosenau, T., Lange, T., Ebner, G., Sixta, H., & Kosma, P. (2020b). A novel method for the determination of carbonyl groups in celluloses by fluorescence labeling. 1. Method development. *Biomacromolecules*, 3(5), 959–968. <https://doi.org/10.1021/bm020029q>
- Selig, M., Vuong, T., Gudmundsson, M., Forsberg, Z., Westereng, B., Felby, C., & Master, E. (2015). Modified cellobiohydrolase–cellulose interactions following treatment with lytic polysaccharide monoxygenase Cels2 (ScLPMO10C) observed by QCM-D. *Cellulose*, 22(4), 2263–2270. <https://doi.org/10.1007/s10570-015-0635-x>
- Shrotri, A., Kobayashi, H., & Fukuoka, A. (2017). Chapter two - Catalytic conversion of structural carbohydrates and lignin to chemicals. *Advances in Catalysis*, 60, 59–123. <https://doi.org/10.1016/bs.acat.2017.09.002>
- Singh, S. (2016). Aspergillus enzymes for textile industry. In V. K. Gupta (Ed.), *New and future developments in microbial biotechnology and bioengineering* (pp. 191–198). Amsterdam: Elsevier. <https://doi.org/10.1016/B978-0-444-63505-1.00014-2>
- Song, B., Li, B., Wang, X., Shen, W., Park, S., Collings, C., Feng, A., Smith, S. J., Walton, J. D., & Ding, S. Y. (2018). Real-time imaging reveals that lytic polysaccharide monoxygenase promotes cellulase activity by increasing cellulose accessibility. *Biotechnology for Biofuels and Bioproducts*, 11, 41. <https://doi.org/10.1186/s13068-018-1023-1>
- Stepnov, A., Forsberg, Z., Sørli, M., Nguyen, G.-S., Wentzel, A., Röhr, Å. K., & Eijsink, V. G. H. (2021). Unraveling the roles of the reductant and free copper ions in LPMO kinetics. *Biotechnology for Biofuels and Bioproducts*, 14, 28. <https://doi.org/10.1186/s13068-021-01879-0>
- Sun, P., Laurent, C. V. F. P., Boerkamp, V. J. P., van Erven, G., Ludwig, R., van Berkel, W. J. H., & Kabel, M. (2021). Regioselective C4 and C6 double oxidation of cellulose by lytic polysaccharide monoxygenases. *ChemSusChem*, 15(2), Article e202102203. <https://doi.org/10.1002/cssc.202102203>
- Tuveng, T. R., Jensen, M. S., Fredriksen, L., Vaaje-Kolstad, G., Eijsink, V. G. H., & Forsberg, Z. (2020). A thermostable bacterial lytic polysaccharide monoxygenase with high operational stability in a wide temperature range. *Biotechnology for Biofuels and Bioproducts*, 13, 194. <https://doi.org/10.1186/s13068-020-01834-5>
- Vaaje-Kolstad, G., Westereng, B., Horn, S. J., Liu, Z., Zhai, H., Sørli, M., & Eijsink, V. G. H. (2010). An oxidative enzyme boosting the enzymatic conversion of recalcitrant polysaccharides. *Science*, 330(6001), 219–222. <https://doi.org/10.1126/science.1192231>
- Vermaas, J., Crowley, M., Beckham, G., & Payne, C. (2015). Effects of lytic polysaccharide monoxygenase oxidation on cellulose structure and binding of oxidized cellulose oligomers to cellulases. *The Journal of Physical Chemistry B*, 119(20), 6129–6143. <https://doi.org/10.1021/acs.jpcc.5b00778>
- Vuong, T., Liu, B., Sandgren, M., & Master, E. (2017). Microplate-based detection of lytic polysaccharide monoxygenase activity by fluorescence-labeling of insoluble oxidized products. *Biomacromolecules*, 18(2), 610–616. <https://doi.org/10.1021/acs.biomac.6b01790>
- Wang, D., Li, Y., Zheng, Y., & Hsieh, Y. (2021). Recent advances in screening methods for the functional investigation of lytic polysaccharide monoxygenases. *Frontiers in Chemistry*, 9, Article 653754. <https://doi.org/10.3389/fchem.2021.653754>
- Wang, S., Lu, A., & Zhang, L. (2016). Recent advances in regenerated cellulose materials. *Progress in Polymer Science*, 53, 169–206. <https://doi.org/10.1016/j.progpolymsci.2015.07.003>
- Westereng, B., Loose, J. S. M., Vaaje-Kolstad, G., Aachmann, F. L., Sørli, M., & Eijsink, V. G. H. (2018). Analytical tools for characterizing cellulose-active lytic polysaccharide monoxygenases (LPMOs). *Methods in Molecular Biology*, 1796, 219–246. https://doi.org/10.1007/978-1-4939-7877-9_16
- Whitmore, P. M., & Bogaard, J. (1994). Determination of the cellulose scission route in the hydrolytic and oxidative degradation of paper. *Restaurator*, 15, 26–45. <https://doi.org/10.1515/rest.1994.15.1.26>
- Zámocký, M., Schümann, C., Sygmund, C., O'Callaghan, J., Dobson, A., Ludwig, R., ... Peterbauer, C. (2008). Cloning, sequence analysis and heterologous expression in *Pichia pastoris* of a gene encoding a thermostable cellobiose dehydrogenase from *Myriococcum thermophilum*. *Protein Expression and Purification*, 59(2), 258–265. <https://doi.org/10.1016/j.pep.2008.02.007>
- Zhou, P., Zhang, J., Zhang, Y., Liu, Y., Liang, J., Liua, B., & Zhang, W. (2016). Generation of hydrogen peroxide and hydroxyl radical resulting from oxygen-dependent oxidation of L-ascorbic acid via copper redox-catalyzed reactions. *RSC Advances*, 6, 38541–38547. <https://doi.org/10.1039/C6RA02843H>
- Zweckmair, T., Oberlerchner, J., Böhmendorfer, S., Bacher, M., Sauerland, V., Rosenau, T., & Pothast, A. (2016). Preparation and characterisation of pure fractions of cellooligosaccharides. *Journal of Chromatography A*, 1431, 47–54. <https://doi.org/10.1016/j.chroma.2015.12.090>